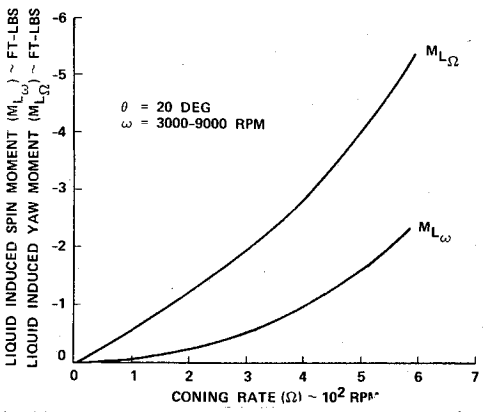

Fig. 3 Liquid induced despin and yawing moment vs coning rate.

Discussion of Results

The dependence of both the liquid induced yawing moment and spin moment with spin rate are similar as shown in Fig. 2. The spin moment was measured for $\dot{\omega} \cong -400$ rpm/s and $\dot{\Omega}=0$; the yaw moment measurement used $\dot{\omega} \cong -320$ rpm/s and $\dot{\Omega}=-6$ rpm/s. Note that both moments increase with spin rate up to about 2500 rpm and then remain fairly constant at higher spin rates. This general dependence was found to be similar for all coning rates. The relative independence of the moments on spin rate at the higher values of spin rate (representative of actual flight conditions) allows both moments to be plotted as a function of coning rate as contained in Fig. 3. This direct proportionality between the yawing moment and despin moment had previously been conjectured, but until now, never demonstrated experimentally.

It should be noted that these data apply specifically to a spin-stabilized artillery projectile. Accordingly, the detailed effect could be different for payload geometries, sizes, and rotational motion associated with other spinning flight vehicles.

The liquid viscosity and coning angle used in these experiments were selected to produce the largest despin and yawing moments possible on the test fixture. However, the results are representative of the phenomenon and provide heretofore unavailable quantitative data for comparison with theoretical predictions.

References

[1] D'Amico, W. P. and Miller, M. C., "Flight Instabilities Produced by a Rapidly Spinning, Highly Viscous Liquid," *Journal of Spacecraft and Rockets,* Vol. 16, Jan.-Feb. 1979, pp. 62-64.

[2] Miller, M. C., "Flight Instabilities of Spinning Projectiles Having Non-Rigid Payloads," *Journal of Guidance, Control, and Dynamics,* Vol. 5, March-April 1982, pp. 151-157.

[3] Miller, M. C., "Void Characteristics of a Liquid Filled Cylinder Undergoing Spinning and Coning Motion," *Journal of Spacecraft and Rockets,* Vol. 18, May-June 1981, pp. 286-288.

[4] D'Amico, W. P. and Roger, T. H., "Yaw Instabilities Produced by Rapidly Rotating, Highly Viscous Liquids," AIAA Paper 81-0224, Jan. 1981.

[5] Murphy, C. H., "Liquid Payload Roll Moment Induced by a Spinning and Coning Projectile," AIAA Paper 83-2142, Aug. 1983.

[6] Vaughn, H. R., Oberkampf, W. L., and Wolfe, W. P., "Numerical Solution for a Spinning Nutating, Fluid-Filled Cylinder," Sandia, National Laboratories, SAND 83-1789, Dec. 1983.

[7] Herbert, T., "The Flow of Highly Viscous Fluid in a Spinning and Nutating Cylinder," *Proceedings of the 1983 Scientific Conference on Chemical Defense Research,* CRDC-SP-84014, Oct. 1984.

[8] Miller, M. C., "Experimental Facilities of the Aerodynamics Research and Concepts Assistance Section," Chemical Systems Laboratory Special Publication, ARCSL-SP-83007, Feb. 1983.

[9] Vaughn, H. R., "A Detailed Development of the Tricyclic Theory," Sandia National Laboratories, SC-M-67-2933, Feb. 1978.

Computerized Generation of Symbolic Equations of Motion for Spacecraft

Edwin J. Kreuzer* and Werner O. Schiehlen†
University of Stuttgart
Stuttgart, Federal Republic of Germany

Introduction

FOR real-time simulations of spacecraft interfacing with hardware, the application of numerical formalisms is restricted due to the required computation time. Therefore, computer programs for the automatic generation of symbolic equations of motion for spacecraft have been developed, e.g., Macala[1] and Rosenthal and Sherman.[2] However, from an engineering point of view, it may be more efficient to extend an existing well-documented and thoroughly tested terrestrial multibody formalism to include spacecraft.

A formalism for the generation of symbolic equations of motion of terrestrial multibody systems have been presented in Ref. 3. The NEWEUL program based on this formalism has provided its high reliability for many technical applications, and can also be extended to orbiting spacecraft.[4] The necessary dynamical background is given herein.

Dynamics of Multibody Systems

In Eq. (25) of Ref. 3, the Newton-Euler equations of a system of p rigid bodies with f degrees of freedom are summarized as

$$\bar{M}(y,t)\ddot{y}+\bar{k}(y,\dot{y},t)=\bar{q}^e(y,\dot{y},t)+\bar{Q}(y,t)g \tag{1}$$

where y is the $f\times 1$ vector of generalized coordinates, and $\bar{M}$ is a $6p\times f$ inertia matrix given by

$$\bar{M}=\bar{\bar{M}}\bar{J} \tag{2}$$

Furthermore, the $6p\times 6p$ block-diagonal matrix of masses m_i and inertia tensors I_i is

$$\bar{\bar{M}}=\mathrm{diag}\{m_1E,\ldots,m_pE,\quad I_1,\ldots,I_p\} \tag{3}$$

with the 3×3 identity matrix E, and the global $6p\times f$ Jacobian matrix

$$\bar{J}=[J_{T1}^T,\ldots,J_{Tp}^T,\quad J_{R1}^T,\ldots,J_{Rp}^T]^T \tag{4}$$

is composed of $3\times f$ Jacobian matrices J_{Ti} and J_{Ri} of translation and rotation. The $6p\times 1$ vectors $\bar{k}$ and $\bar{q}^e$ describe the gyroscopic and applied forces, respectively. The $6p\times q$ distribution matrix $\bar{Q}$ assigns the $q\times 1$ vector g of generalized constraint forces to each body of the system. Application of Lagrange's form of D'Alembert's principle leads to a premultiplication of Eq. (1) with $\bar{J}^T$ and results in the complete elimination of all constraint forces. Then, the equations of motion are given by the $f\times 1$ second-order vector differential equation

$$M(y,t)\ddot{y}+k(y,\dot{y},t)=q(y,\dot{y},t) \tag{5}$$

Presented as Paper 83-302 at the AAS/AIAA Astrodynamics Specialist Conference, Lake Placid, N.Y., Aug. 22-25, 1983; received Sept. 15, 1983; revision received Feb. 6, 1984.

*Assistant Professor, Institute B of Mechanics.
†Professor, Institute B of Mechanics. Member AIAA.

where M is a symmetric, positive-definite $f\times f$ inertia matrix, and k and q are $f\times 1$ vectors of generalized gyroscopic and applied forces. Equation (5) describes the motion of the system in terms of the minimal number of differential equations. For many technical applications, the linearized equation of motion

$$M\ddot{y}+(D+G)\dot{y}+(K+N)y=h(t) \tag{6}$$

is sufficient. Here the symmetrical $f\times f$ matrices M, D, and K describe inertia, damping, and stiffness, the skew-symmetrical $f\times f$ matrices G and N represent gyroscopic and circulatory forces, and $h(t)$ is the $f\times 1$ excitation vector.

Dynamics of Orbiting Multibody Systems

The dynamics of spacecraft in orbit usually are described with respect to a moving reference frame tied to the center of mass of the system. Then, the rotational and internal motion of the spacecraft are easily separated from the motion of the origin of the reference frame (center of mass). Standard celestial mechanics may be used to obtain the motion of the center of mass, independent of the remaining equations of attitude dynamics. The separation method will be presented next.

Consider the spacecraft shown in Fig. 1 modeled as a multibody system. The vector of generalized coordinates is decomposed as

$$y=[y_b^T\,|\,y_r^T]^T \tag{7}$$

where y_b is a 3×1 vector of inertial coordinates describing the origin of the basebody, and y_r is a $(f\text{-}3)\times 1$ vector of remaining coordinates.

In an orbiting multibody system, the total of all constraint forces vanishes. Introducing the $3\times 6p$ summation matrix

$$\bar{E}=[E_1\ldots E_p\,|\,0\ldots 0] \tag{8}$$

of 3×3 identity and zero matrices leads to

$$\bar{E}\bar{Q}g=0 \tag{9}$$

characterizing the vanishing total of all external constraint forces. Furthermore, the decompositon of the vector y in accordance with Eq. (7) yields a corresponding decomposition of matrix (4):

$$\bar{J}=[\bar{E}^T\,|\,\bar{J}_r] \tag{10}$$

where $\bar{J}_r$ is a $6p\times(f-3)$ Jacobian matrix representing the internal constraints of the orbiting multibody system.

All that remains to be done is to express Eq. (1) by means of Eq. (10) and apply D'Alembert's principle for the elimination of internal constraint forces and torques.

To begin, the equations for y_b read as

$$m\ddot{y}_b+\bar{E}\bar{M}\bar{J}_r\ddot{y}_r+\bar{E}\bar{k}=\bar{E}\bar{q}^e \tag{11}$$

where

$$m=\sum_{i=1}^{p} m_i \tag{12}$$

The acceleration $\ddot{y}_b$ of the basebody is obtained in terms of $\ddot{y}_r$ as

$$\ddot{y}_b=(1/m)\bar{E}(\bar{q}^e-\bar{k}-\bar{M}\bar{J}_r\ddot{y}_r) \tag{13}$$

The remaining equation

$$\bar{J}_r^T[\bar{M}(\bar{E}^T\ddot{y}_b+\bar{J}_r\ddot{y}_r)+\bar{k}]=\bar{J}_r^T\bar{q}^e \tag{14}$$

depends also on $\ddot{y}_b$ and $\ddot{y}_r$, however, $\ddot{y}_b$ can be replaced byEq. (13). After this operation, one arrives at the following reduced system of $(f-3)$ differential equations written in matrix form:

$$\tilde{M}(y_r,t)\ddot{y}_r+\tilde{k}(y_r,\dot{y}_r,t)=\tilde{q}(y_r,\dot{y}_r,t) \tag{15}$$

The $(f-3)\times(f-3)$ mass matrix follows as

$$\tilde{M}=\bar{J}_r^T\bar{M}[\bar{J}_r-(1/m)\bar{E}^T\bar{E}\bar{M}\bar{J}_r] \tag{16}$$

With the $6p\times 6p$ identity matrix $\bar{\bar{E}}$, the $(f-3)\times 1$ vector of gyroscopic forces is

$$\tilde{k}=\bar{J}_r^T[\bar{\bar{E}}-(1/m)\bar{M}\bar{E}^T\bar{E}]\bar{k} \tag{17}$$

and the $(f-3)\times 1$ vector of applied forces reads as

$$\tilde{q}=\bar{J}_r^T[\bar{\bar{E}}-(1/m)\bar{M}\bar{E}^T\bar{E}]\bar{q}^e \tag{18}$$

For small motions of time-invariant systems, Eq. (15) can be linearized, resulting in

$$\tilde{M}\ddot{y}_r+(\tilde{D}+\tilde{G})\dot{y}_r+(\tilde{K}+\tilde{N})y_r=\tilde{h}(t) \tag{19}$$

where the symmetrical $(f-3)\times(f-3)$ matrices $\tilde{D}$ and$\tilde{K}$ describe damping and stiffness, the skew-symmetrical $(f-3)\times(f-3)$ matrices $\tilde{G}$ and $\tilde{N}$ represent gyroscopic and circulatory forces, and the $(f-3)\times 1$ exitation vector $\tilde{h}(t)$ is introduced.

Equation (15) or (19), respectively, describes the dynamics of an orbiting multibody system. With the formula given in

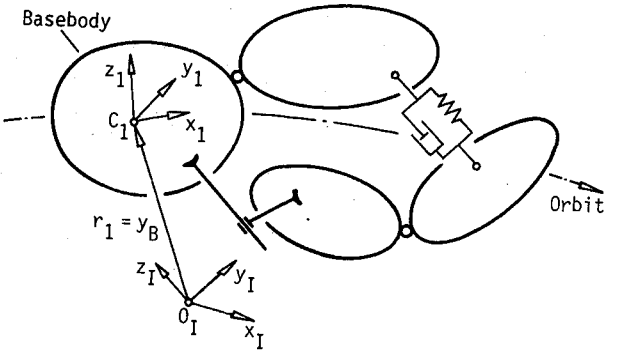

Fig. 1 Orbiting multibody system.

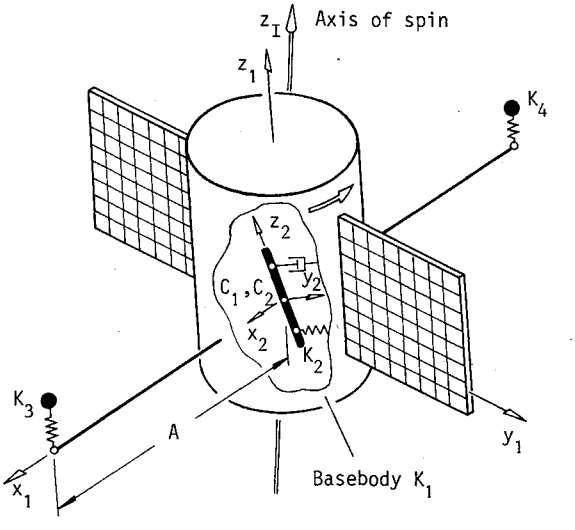

Fig. 2 Spin-stabilized satellite.

this section, formalisms for terrestrial multibody systems may be extended to include spacecraft applications.

The NEWEUL Program

The equations presented herein were implemented using the NEWEUL program for application to orbiting spacecraft. The program is written in FORTRAN. It uses a special coding scheme allowing symbolic equation manipulation to produce a problem-specific FORTRAN code for real-time simulations.

The input required by the NEWEUL program are data describing the kinematical interconnection of rigid bodies, the inertia properties of the bodies, and the applied forces and torques, where

$y = f \times 1$ vector of generalized coordinates
$r_i(y,t) = 3 \times 1$ vector of the center of mass C_i of body i
$S_i(y,t) = 3 \times 3$ rotation matrix of body-fixed frame with respect to an inertial frame
m_i = mass of body i
$I_i = 3 \times 3$ inertia tensor with respect to the center of mass C_i
$f_i^e = 3 \times 1$ vector of applied forces on body i
$l_i^e = 3 \times 1$ vector of applied torques on body i

All these data can be obtained easily from the system under consideration. The transformation of the inertia tensor given with respect to a body-fixed frame into a reference frame can be performed by the program as well as the calculations concerning the applied forces and torques. An interactive dialog system greatly facilitates the entry of all input data, especially the determination of vectors r_i and matrices S_i which is very convenient. There are options for linear or nonlinear equations of motion.

Example

Due to space limitations, only a simple model of a spin-stabilized satellite with nutation damper (Fig. 2) is considered. The model consists of two rigid bodies and two particles: a basebody K_1 and a pendulum K_2 connected to K_1 at point C_1 by a hinge with body-fixed axis. Lines x_i, y_i, z_i $(i=1,2)$ are, respectively, principal axes of inertia of body K_1 and K_2 with respect to their mass centers C_1 and C_2, and x_1 is assumed parallel to x_2. The particles K_3 and K_4 are mounted on flexible, massless beams along the x_1 axis of the basebody. The following generalized coordinates describe the system.

```
MG=M1+M2+2.*M3
MGI=1./MG

M(1,1)=IX1+IX2
M(1,3)=IX2
M(2,2)=2.*A**2*M3+IY1+IX2
M(2,4)=-A*M3
M(2,5)=A*M3
M(3,3)=IX2
M(4,4)=-M3**2*MGI+M3
M(4,5)=-M3**2*MGI
M(5,5)=-M3**2*MGI+M3

D(3,3)=D1

G(1,2)=-OM*IX1-OM*IY1+IZ1*OM-2.*OM*IX2
G(2,1)=OM*IY1+OM*IX1-IZ1*OM+2.*OM*IX2
G(2,3)=2.*OM*IX2
G(3,2)=-2.*OM*IX2

K(1,1)=-OM**2*IY1+IZ1*OM**2-OM**2*IX2
K(1,3)=-OM**2*IX2
K(2,2)=2.*OM**2*A**2*M3-OM**2*IX1+IZ1
      *OM**2-OM**2*IX2
K(2,4)=-OM**2*A*M3
K(2,5)=OM**2*A*M3
K(3,3)=-OM**2*IX2+C1
K(4,4)=C2
K(5,5)=C3
```

Fig. 3 Listing of the equations of motion.

PHI,TET = angles of basebody K_1 with respect to the inertial spin axis
DEL = angle of pendulum K_2 with respect to K_1
XI, ETA = displacement of masspoint K_3, K_4 parallel z_1 with respect to K_1

All angles and displacements are assumed to be small. The position of the center of mass of the basebody with respect to an inertial frame is described by three inertial coordinates, summarized in $y_b = [X\ Y\ Z]^T$. The basebody is rotating with constant angular velocity OM*T around z_1. Thus, the system has eight degrees of freedom.

The input data for the NEWEUL program are specified as follows:

Generalized coordinates

$$y = [y_b^T | y_r^T]^T = [X\ Y\ Z\ |\ \text{PHI TET DEL XI ETA}]^T$$

Rotation matrices

$$S_1 = S_1(\text{PHI,TET,OM*}T), \quad S_2 = S_2(S_1, \text{DEL})$$

Vectors of center of mass

$$r_i = \begin{bmatrix} X \\ Y \\ Z \end{bmatrix} \quad i = 1,2$$

$$r_3 = r_1 + S_1 \begin{bmatrix} A \\ O \\ XI \end{bmatrix}, r_4 = r_1 + S_1 \begin{bmatrix} -A \\ O \\ ETA \end{bmatrix}$$

where A is shown in Fig. 2.

Masses

$$m_i = M_i, \quad i = 1,\ldots,4, \quad m_3 = m_4$$

Inertia tensors with respect to frame x_1, y_1, z_1

$$I_1 = \begin{bmatrix} IX1 & O & O \\ O & IY1 & O \\ O & O & IZ1 \end{bmatrix}$$

$$I_2 = \begin{bmatrix} IX2 & O & O \\ O & IX2 & DEL*IX2 \\ O & DEL*IX2 & O \end{bmatrix}, \quad I_3 = I_4 = O$$

where IX1, IY1, IZ1, and IX2 are principal moments of inertia. Due to the spin stabilization there are only internal applied forces depending on spring constants C1, C2, C3 and the damping coefficient D1.

From these data, the extended NEWEUL program generates the linearized equations of motion [Eq. (19)]. The listing of the output produced by the program is shown in Fig. 3. Only the essential elements different from O are listed.

Conclusion

This Note describes the extension of formalisms, originally developed for the computerized generation of equations of motion of terrestrial multibody systems, to orbiting spacecraft. It is shown how the translational motion of the system's basebody can be separated from the rotational and internal motion. The method is applied to NEWEUL, a program for generation of symbolic equations of motion of terrestrial mutlibody systems. An example shows the input data and the symbolic equations of motion explicitly.

References

[1]Macala, G.A., "SYMBOD: A Computer Program for the Automatic Generation of Symbolic Equations of Motion for Systems of Hinge-Connected Rigid-Bodies," AIAA Paper 83-013, Jan. 1983.

[2]Rosenthal, D.E. and Sherman, M.A., "Symbolic Multibody Equations via Kane's Method," AIAA Paper 83-303, Aug. 1983.

[3]Schiehlen, W.O. and Kreuzer, E.J., "Symbolic Computerized Derivation of Equations of Motion," *Dynamics of Multibody Systems,* edited by K. Magnus, Springer-Verlag, Berlin, 1978, pp. 290-305.

[4]Kreuzer, E.J. and Schiehlen, W.O., "Generation of Symbolic Equations of Motion for Complex Spacecraft Using Formalism NEWEUL," AIAA Paper 83-302, Aug. 1983.

A Relation Between Liquid Roll Moment and Liquid Side Moment

Charles H. Murphy*
Ballistic Research Laboratory
Aberdeen Proving Ground, Maryland

Introduction

IN the summer of 1974, a 155-mm shell with a liquid payload was fired with a yawsonde telemetry unit. This projectile developed a large amplitude coning motion. When the coning motion exceeded forty deg, the telemetry record showed a very rapid despin of 40% in less than five s.[1] Since 1974, ten more observations of large coning motions and large despin rates of liquid-filled projectiles have been made.[2-4] In addition, 36 observations have been made of large coning motions and despin moments for projectiles with payloads of liquid-solid mixtures.[5] Indeed, all projectiles with liquid or liquid-solid payloads were observed to perform large coning motion and to experience large losses in spin.

This characteristic association of a large despin moment with a large coning motion for a projectile with a moving payload can become a diagnostic tool. Miller[6] suggested using this tool to determine the existence of small-amplitude, unstable, liquid-induced side moments. Spin measurements made during coning motion on a gyroscope predicted flight pitch instaiblities caused by very viscous liquids. These were observed in flight.[7]

The linear liquid-induced side moment was first computed by Stewartson[8] for an inviscid liquid payload by use of eigenfrequencies determined by the fineness ratio of the cylindrical container. Wedemeyer[9] introduced boundary layers on the walls of the container and was able to determine viscous corrections for Stewartson's eigenfrequencies, which could then be used in Stewartson's side moment calculation. Murphy[10] then completed the linear boundary layer theory by including all pressure and wall shear contributions to the liquid-induced side moment.

The first theoretical work on liquid-induced roll moments was done by Vaughn[11] in 1978. Although fair agreement was obtained with Miller's data, the work was marred by some hard-to-justify algebraic steps. Recently Vaughn et al.[12] developed an impressive numerical capability for computing roll moments of very high viscosity liquids and obtained excellent agreement with Miller's data. In Ref. 5, the linearized Navier-Stokes equations were used to develop a relationship between the liquid side moment and the liquid roll moment. This relationship can be used to predict the side moment from a measured roll moment. It is the purpose of this Note to give the results of this analysis and illustrate its predictions with yawsonde data recently analyzed by Pope.[13]

Submitted Feb. 10, 1984; revision received April 30, 1984. This paper is declared a work of the U.S. Government and therefore is in the public domain.

*Chief, Launch and Flight Division. Fellow AIAA.

Liquid Roll Moment

Two coordinate systems will be used in this Note: 1) the nonrolling aeroballistic $\bar{X}\bar{Y}\bar{Z}$ system whose $\bar{X}$-axis is fixed along the missile's axis of symmetry, and 2) the inertial XYZ system whose X-axis is tangent to the trajectory at time zero. Both coordinate systems have origins at the center of the cylindrical payload cavity, which is assumed to be at the center of mass of the projectile.

Although the general motion of a spinning projectile is the sum of two coning motions,[10] in this Note we will restrict ourselves to a single coning motion with amplitude α_c and phase angle ϕ_c. In terms of this coning motion, the liquid transverse moment and liquid roll moments must be odd and even functions of α_c, respectively, and are assumed to have the form

$$M_{L\bar{Y}} + iM_{L\bar{Z}} = m_L a^2 \dot{\phi}^2 \tau (C_{\mathrm{LSM}} + iC_{\mathrm{LIM}}) K_c e^{i\phi_c} \quad (1)$$

$$M_{L\bar{X}} = m_L a^2 \dot{\phi}^2 [C_{\mathrm{LRM}_0} + \tau K_c^2 C_{\mathrm{LRM}}] \quad (2)$$

where m_L is the mass of liquid in a fully filled container, a is the maximum radius of the container, $\dot{\phi}$ is the spin rate, τ is the ratio of coning rate to spin rate, $\dot{\phi}_c/\dot{\phi}$, C_{LSM} is the liquid side moment coefficient, C_{LIM} is the liquid in-plane moment coefficient, and K_C is $\sin \alpha_c$.

When the liquid has reached a steady-state rolling and coning motion, the roll moment must vanish in the absence of coning motion. Thus C_{LRM} is the steady-state liquid roll moment coefficient due to coning motion while C_{LRM_0} is the

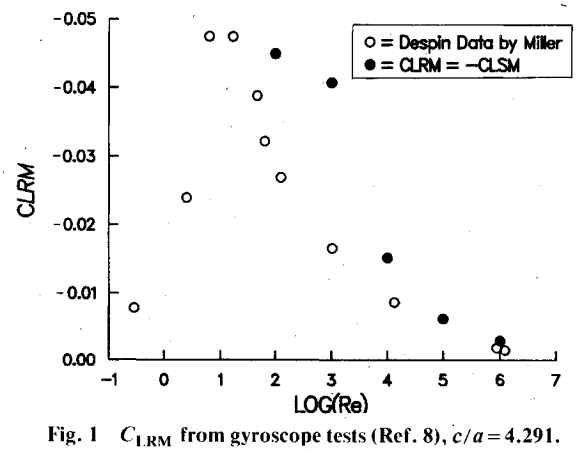

Fig. 1 C_{LRM} from gyroscope tests (Ref. 8), $c/a = 4.291$.

Table 1 Pope's results

Yawsonde	Re	τ	C_{LRM}	C_{SMEQ}	C_{SMA}
404[a]	2×10^6	0.090	−0.05	0.05	<0.01
1339	1.8×10^6	0.090	−0.02	0.04	−0.005
1866	45.2	0.123	−0.055	0.050	−0.004
1867	45.2	0.123	−0.055	0.050	−0.004
1868	45.2	0.123	−0.060	0.053	−0.004
1955	20	0.087	−0.04	0.04	−0.010
1293	10	0.090	−0.03	0.02	−0.008
1313	10	0.088	−0.02	0.025	−0.008
1585	10	0.091	−0.025	0.02	−0.008
1587	10	0.093	−0.04	0.02	−0.008
1588	10	0.095	−0.03	0.02	−0.008
1693[b]		0.094	−0.025	0.025	−0.005

[a]Fill ratio for 404 was 87%; all others were 100%. [b]This projectile contained white phosphorous-impregnated felt wedges.[14]